



# Performance Improvement of an Integrated Collector Storage Solar Water Heater by Using an Additional Glass Cover: A Numerical Study

<sup>1</sup>Angham F. Abed, <sup>1</sup>Noora A. Hashim\*, <sup>2</sup>Ruaa B. Dahham, <sup>1</sup>Esam H. Alkaldy

<sup>1</sup>Department of Mechanical Engineering, Faculty of Engineering, University of Kufa, Iraq

<sup>2</sup>School Buildings Division, Najaf Education Directorate, Ministry of Education, Iraq

## Article information

### Article history:

Received: October, 30, 2023

Accepted: January, 12, 2024

Available online: October, 20, 2024

### Keywords:

Rectangular solar storage,  
Collector,  
COMSOL,  
Collector thermal efficiency

### \*Corresponding Author:

Noora A. Hashim  
[nooraa.alkhalidi@uokufa.edu.iq](mailto:nooraa.alkhalidi@uokufa.edu.iq)

### DOI:

<https://doi.org/10.53523/ijoirVol11I2ID384>

This article is licensed under:

[Creative Commons Attribution 4.0 International License](https://creativecommons.org/licenses/by/4.0/).

## Abstract

This paper describes the analysis of a solar storage water heating system, emphasizing its cost-effectiveness and integrated design. The study employs numerical analysis to assess and optimize the performance of a rectangular solar collector with an added glass cover and an internal horizontal barrier. Using COMSOL software, a three-dimensional modeling study was conducted in the Kufa-Najaf climate on May 9th. The analysis focused on fundamental convection equations governing mass, momentum, and energy conservation. Temperature and velocity distributions were obtained at 13:30 PM, revealing a peak storage water temperature of 56.3 °C. The additional glass cover-barrier storage collector, set at a 60° angle, exhibited the highest stored energy at 2065.6 W, surpassing the conventional storage collector at 1007.06 W. Furthermore, the model demonstrated an increased instantaneous efficiency of 58.3%, compared to 28.4% for the conventional collector. The simulation results align well with previous findings, showing a maximum mean absolute percent error (MAE) of 4.5%.

## 1. Introduction

Renewable energy sources must quickly replace current energy sources like nuclear power and fossil fuels in order for evolution to be sustainable. This is because renewable energy sources are environmentally friendly, sustainable, and have the capacity to meet both present and future global energy demands without posing any harm to the environment [1]. One of the main uses of solar energy is for the heating of water. The most important consideration when building any solar collector is to ensure that the absorber portion of the collection receives the maximum amount of solar energy while also minimizing heat losses from the absorber. The abundant solar energy that is beaming over the region and freely available every day is a blessing for other tropical nations. One effective method of absorbing solar energy is to use a device called a "collector" to considerably elevate the water's temperature [2]. Numerous uses need for hot water, and special devices called solar water heaters make it possible to heat water efficiently and affordably using solar energy [3]. One of the most effective and affordable solar energy devices available today is the solar heater. The solar heating system is

distinguished by its ease of manufacture, simple installation and no requirement for costly maintenance procedures. The three main parts of a solar heater are the collecting and preservation tank, the connecting pipes, and the solar collector [4]. Solar water heaters (SWHs) are often divided into three categories: natural (free), forced convection, and at last (under investigation), integrated- collector storage solar water heaters (ICSSWH) that are the most affordable and straightforward to construct because they have no moving parts [5, 6]. The integrated ICSSWH has many benefits over the alternative variants. Firstly because of the absent of any significant heat losses from water circulation during the day which ensure good efficiency. Secondly, compared to forced and natural convections, which have limited bond conductance, the large surface area of contact between the absorber plate and the water allows for superior heat transfer. Finally, it is produced using inexpensive materials and simple manufacturing techniques without the need of advanced technology [7]. Using a rectangle collector, Joudi, Hussein, and Farhan [8] suggested redesigning a solar storage collector for home hot water delivery. It is made to work as a storage tank and collector inside a component. Over the previous models, their new one model boasted a number of benefits. It was effective since there were no losses of heat

During circulation of water through the day. With the use of ANSYS software, Ahmed et al. [9] conducted an analysis of the rectangular storage collector. The studies most important scientific finding is that the absorbent plate's ratio to storage volume must not be less than 12. Experimental research on the effectiveness of a triangle solar collector was conducted by Ahmed in 2018 [10]. The sunny portion is painted with black glass, or the slope side facing the sun might be covered with another transparent material to improve solar energy absorption. Thermal insulation insulates all other surfaces. The experimental research showed that in November, the tank's average temperature reached 40 °C. Their study intended to develop a low-cost, dependable, and efficient solar water heating system for domestic use. An analysis of a cylindrical storage collector using both empirical and theoretical methods was conducted by Khalil Ahmed [11]. It had been proposed to cut a cylinder in an inclined cut plane. The effects of hot water removal throughout summer and winter weather conditions were tested. In the cylindrical collector, the maximum range of the average storage temperature was 25 °C. A typical spring day had a temperature profile of 58 °C at the tip of the cylindrical header. The intended solar collector's performance was largely on par with conventional flat-plate solar water heaters. In order to show the practicality of a solar storage collector for household use, Omer Khalil Ahmed [12] proposed a redesign of one. The wedge collector is the name given to this unique collector. It can be used as a reservoir to store water instead of the standard cubic or cylindrical container used for household purposes. Based on the research, a storage collector is created by cutting a two-plane cylinder into one with a vertical first plane and one with a 45° slope on the other. Mokhlif et al.'s experimental study [13] examined how well ICS-SWHs function when used with a reflector-insulator cover. Insulation was added to the rear of the reflectors so that they could serve as both coverings and reflectors. The findings demonstrated that, in comparison to the ICS-SWH without insulated reflectors, the latter's thermal efficacy had increased by 23%. Furthermore, the stored water might become as high as 82 °C during the day and 46 °C in the morning on the coldest day. Mokhlif et al.'s experimental research [14] centered on a dual glazing cover and corrugated absorber plate ICS-SWH system. Studies were done to find out how the performance of the ICS-SWH was affected by the dual glazing cover. On the first morning of the second and third days, storage water temperatures in situations with dual glazing covers were found to be 6 and 11 °C higher than those in scenarios with single glazing covers. The built-in regime's mass flow rate was 0.0091 kg/s, and its average daily thermal efficacy was 68%. Compared to a single-glazing cover, a dual-glazing cover showed a 4.6% higher daily thermal efficacy. Following an examination of the previously stated literature. The impacts of the variable internal barrier's inclination angle and an additional glass cover with a closed air space on the rectangular Integrated Collector-Storage (ICS) solar water heater were discovered to have garnered little attention. The primary target of the current study is to employ a three-dimensional, unsteady model to demonstrate how a dual-glazing cover with internal horizontal partition can be used in order to enhance the functionality of a rectangle integrated storage solar collector. Due to a restricted air between them, heat transfer to the surrounding area is decreased by a double glass cover. The second goal of this research endeavor is to investigate how modifying the barrier's inclination angle and environmental factors affects the operational parameters of the collector.

## 2. Numerical Models

The storage tank and the solar collector are the two basic components of traditional solar water heaters. Due to the integration of solar collectors and storage tanks into one component, a solar storage collector differs from a typical collector. A wooden box with insulation and a sheet of glass on top of the box to create an air gap to trap

solar energy is the basic design for the integrated storage solar collector. It has a sunny surface that is painted black to maximize solar radiation absorption. The rectangular solar storage collector with a double glass cover and internal barrier was given a numerical evaluation in this paper. Figure (1) depicts the schematic configurations for the modified rectangular storage solar collector tank in three-dimensions (3D). In the first model, conventional storage collectors are utilized. Additionally, a glass cover with an internal barrier is utilized in the other type, which has a variable inclination angle ( $\theta = 0^\circ$  horizontal,  $30^\circ$ ,  $60^\circ$ ,  $90^\circ$  no barrier) and measures  $L_b$  0.4m in length and  $H_b$  0.2m in height. Staying within the permitted range for solar collectors, the absorber plate was spaced 45 mm from the glass's bottom, which sloped upward at a 45-degree angle [15]. The 0.02 m deep additional enclosed air space [16]. The walls were insulated on both the horizontal and vertical sides.

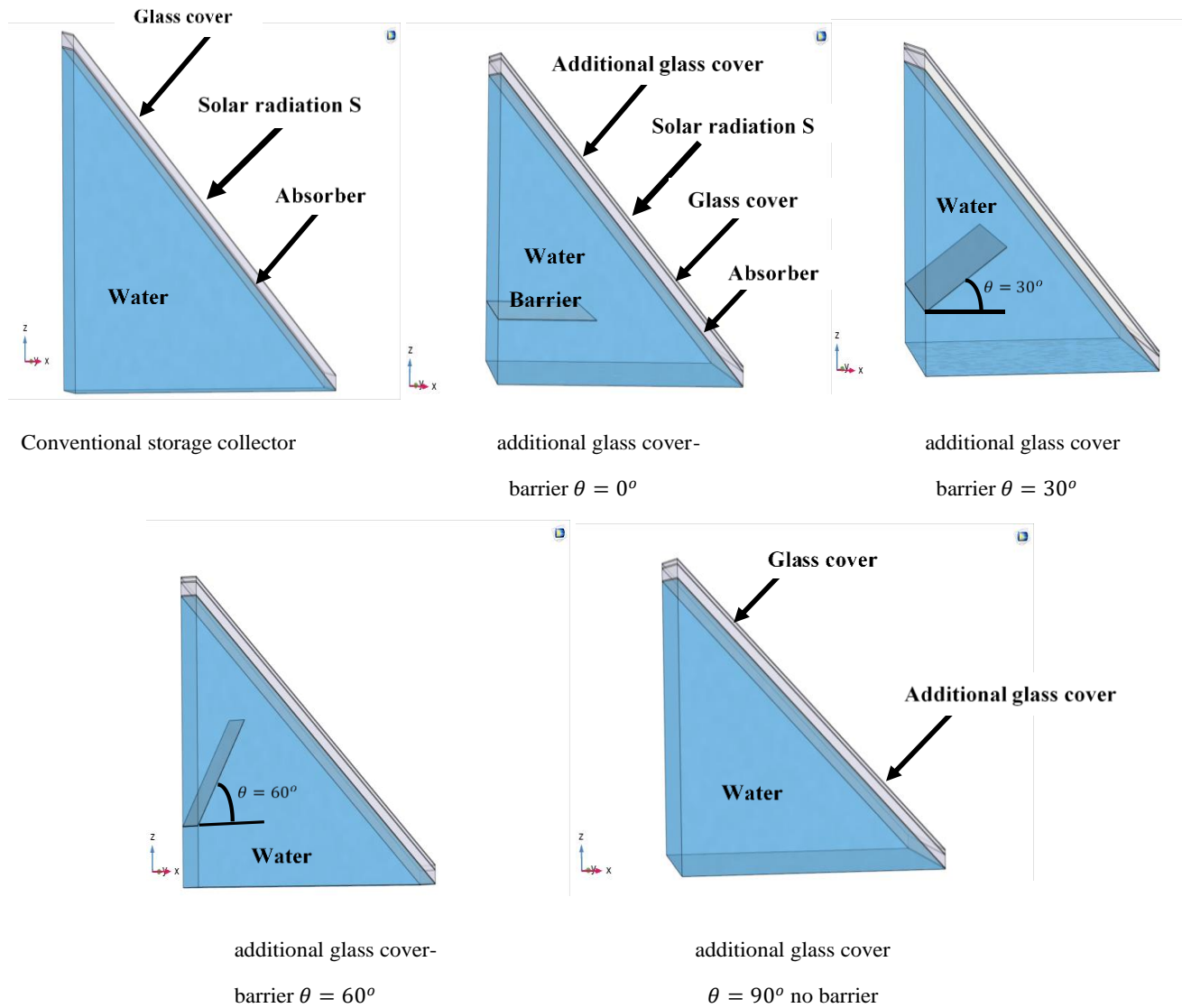


**Figure (1):** Diagram for the suggested solar storage collector models.

### 3. Governing equations

Natural convection problems are caused by fluid motion due to heat transfer. In the Boussinesq approximation, the fluid density is taken to be constant, assuming that the fluid is Newtonian and incompressible except for the effect of density changes in creating buoyant forces. The effects of viscous energy dissipation are ignored since it is more practical to see the fluid motion as laminar, three-dimensional, and without internal heat generation. The fundamental convection equations under these presumptions are: Equation of Continuity [17]:

$$\frac{\partial \rho}{\partial t} + \frac{\partial u}{\partial x} + \frac{\partial v}{\partial y} + \frac{\partial w}{\partial z} = 0 \quad (1)$$

Where  $u, v, w$  is the velocity in x, y, z directions (m/s), and  $\rho$  is the density of flow [kg/m<sup>3</sup>].

Equations of Momentum [17]. In x-direction:

$$\rho \left( \frac{\partial u}{\partial t} + u \frac{\partial u}{\partial x} + v \frac{\partial u}{\partial y} + w \frac{\partial u}{\partial z} \right) = \rho g_x - \frac{\partial P}{\partial x} + \mu \left( \frac{\partial^2 u}{\partial x^2} + \frac{\partial^2 u}{\partial y^2} + \frac{\partial^2 u}{\partial z^2} \right) \quad (2)$$

In y-direction:

$$\rho \left( \frac{\partial v}{\partial t} + u \frac{\partial v}{\partial x} + v \frac{\partial v}{\partial y} + w \frac{\partial v}{\partial z} \right) = \rho g_y - \frac{\partial P}{\partial y} + \mu \left( \frac{\partial^2 v}{\partial x^2} + \frac{\partial^2 v}{\partial y^2} + \frac{\partial^2 v}{\partial z^2} \right) \quad (3)$$

In z-direction:

$$\rho \left( \frac{\partial w}{\partial t} + u \frac{\partial w}{\partial x} + v \frac{\partial w}{\partial y} + w \frac{\partial w}{\partial z} \right) = \rho g_z - \frac{\partial P}{\partial z} + \mu \left( \frac{\partial^2 w}{\partial x^2} + \frac{\partial^2 w}{\partial y^2} + \frac{\partial^2 w}{\partial z^2} \right) \quad (4)$$

Equation of Energy [17]:

$$\rho C_p \left( \frac{\partial T}{\partial t} + u \frac{\partial T}{\partial x} + v \frac{\partial T}{\partial y} + w \frac{\partial T}{\partial z} \right) = K \left( \frac{\partial^2 T}{\partial x^2} + \frac{\partial^2 T}{\partial y^2} + \frac{\partial^2 T}{\partial z^2} \right) \quad (5)$$

Where: P is the fluid's pressure [Pa], and  $\mu$  is the fluid's dynamic viscosity [N.s/ m<sup>2</sup>],  $C_p$  is a specific heat of fluid [J/kg K], and K is a thermal conductivity of fluid [W/m.K]. The physical-thermal properties of water are listed in Table (1) [18]. Figure (2) illustrates the proper boundary conditions for the proposed storage solar collector model. Where:

$Q_{absor}$	Solar energy absorbed by the absorber surface and equal to $(S \cdot A_a \cdot \tau_{ag} \cdot \tau_g \alpha_{absor})(W)$
$Q_{ag}$	Solar energy incident on transparent additional glass cover and equal to $(S \cdot A_a \cdot \alpha_{ag})(W)$
$Q_g$	Solar energy incident on transparent glass cover and equal to $(S \cdot A_a \cdot \alpha_g \cdot \tau_{ag})(W)$
$Q_{cam}$	Convective heat losses to ambient and equal to $(h_{cam}(T_{ag} - T_{am}))$ [W/m <sup>2</sup> ]
$Q_{rsk}$	Radiation heat losses to sky and equal to $(0.9 \times \sigma \times \varepsilon \times (T_{ag}^4 - T_{sk}^4))$ [W/m <sup>2</sup> ]
$Q_{st}$	Storage energy gain [W]
$h_{cam}$	Convective heat transfer coefficient to ambient and equal to $(2.8 + 3.3v_{wi})$ [W/m <sup>2</sup> .K]
$S$	The total amount of solar radiation on an inclined surface [W/m <sup>2</sup> ]
$A_a$	The absorber's inclined surface area [m <sup>2</sup> ]
$\tau_{ag}$	The additional glass cover's transmissivity [-]
$\tau_g$	Glass cover's transmissivity [-]
$\alpha_{absor}$	Absorption coefficient of absorber plate [-]
$\alpha_{ag}$	Absorptivity of additional glass surface
$\alpha_g$	Absorptivity of glass surface
$h_{cam}$	Convective heat transfer coefficient to ambient and equal to $(2.8 + 3.3v_{wi})$ [W/m <sup>2</sup> .K]
$v_{wi}$	Wind speed (m/s)
$T_{ag}$	Additional glass cover's temperature [°C]
$T_{am}$	Temperature of ambient [°C]
$T_{sk}$	Sky temperature [°C]
$\sigma$	Stefan-Boltzmann constant
$\varepsilon$	Glass emittance [-]

**Table (1):** Water's thermophysical characteristics [18].

<i>Quantity</i>	<i>Expression</i>
Density (kg/ m <sup>3</sup> )	$\rho = 1001 - 0.08832 * T - 0.003417 * T^2$
Specific heat (J/kg K)	$C_p = 4226 - 3.224 * T + 0.0575 * T^2 - 0.0002656 * T^3$
Thermal conductivity (W/m K)	$K = 0.557 + 0.002198 * T^1 - 0.00000708 * T^2$
Kinematic viscosity (m <sup>2</sup> /s)	$\nu = \left(\frac{1}{0.5155+0.0192T} + 0.12\right) * 10^{-6}$

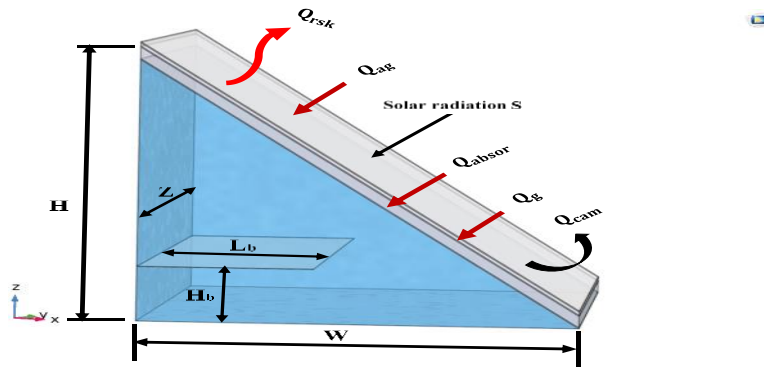


**Figure (2):** The geometric shape and heat transfer types of the suggested model.

#### 4. Grid Dependence Test

For each of the analyzed configurations in this work, a thorough mesh testing was carried out in order to quantify and evaluate the grid-dependency test and ensure a grid-independent solution. By calculating out the average storage water temperature inside the solar storage collector shown in Figure (1), the grid independence test was evaluated. For the current models in the computational domain, meshing using finite elements is carried out; and the additional glass cover-barrier storage collector with  $\theta=0^\circ$  and conventional storage collector models are seen in Figure (3). In the numerical model that is currently in use, the subdomain and boundary elements have been selected as free triangular form with the following elements for additional glass cover-barrier storage collector with  $\theta=60^\circ$ : 105621, 160671, 218867, 386075, 505598, 1378488 and for conventional storage collector: 35404, 54590, 76018, 197809, 719366 and the outcomes are shown in Table (2). It is evident that a grid mesh domain element with (505598 and 197809) respectively are taken into account for additional glass cover storage collector and conventional storage collector in the numerical analysis, which is adequate to depict the phenomena of fluid flow and heat transfer inside the collector. Regarding the featured table, additional grid point increments yield identical outcomes in water temperature.

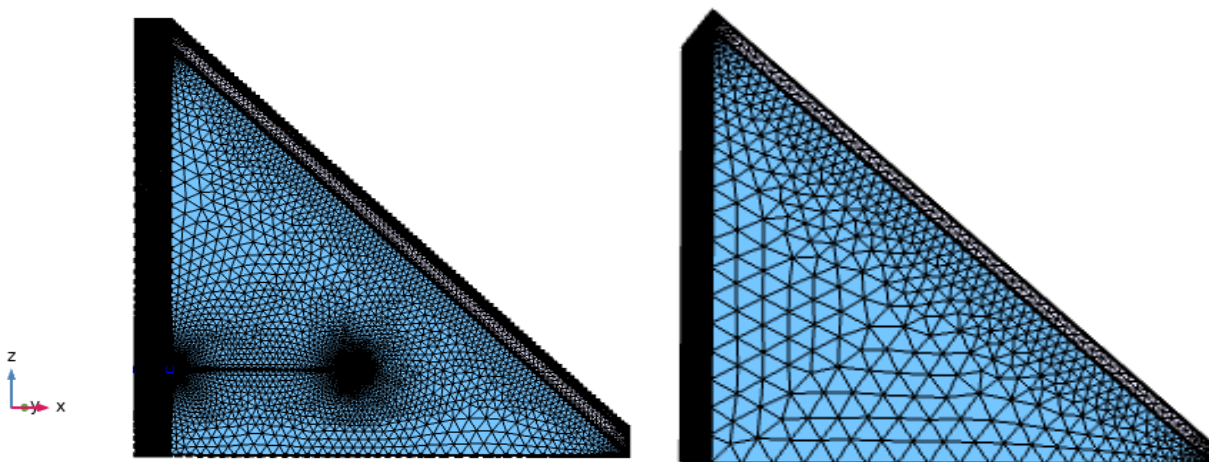


**Figure (3):** Grid-dependency check of the suggested models.

**Table (2):** Grid sensitivity Check for the numerical simulation.

Type of meshing	coarser	coarse	normal	fine	finer	extra finer
additional glass cover-barrier storage collector with $\theta=60^\circ$						
Elements	105621	160671	218867	386075	505598	1378488
Average water storage temperature( $^\circ\text{C}$ )	45.77	46.48	47.23	47.68	47.79	47.79
conventional storage collector						
Elements	35404	54590	76018	197809	719366	
Average water storage temperature( $^\circ\text{C}$ )	38.13	38.50	39.17	39.19	39.19	

### 5. Validation of the Results

A comparison of the current findings with Ahmad's [19] experimental findings for a conventional solar storage collector is shown in Figure (4). Our model for the three-dimensional simulation is utilized to assess and contrast the temperature of the storage water of the collector under the climatic parameters of the experimental investigation [19] for this comparative arrangement. The results of the Ahmad experiment [19], with a mean absolute percent error (MAE) = 4.5%, clearly show that the average temperature of storage achieves a maximum amount prior starting to decrease around 3 PM. The current simulation model and previous findings have a good level of agreement.

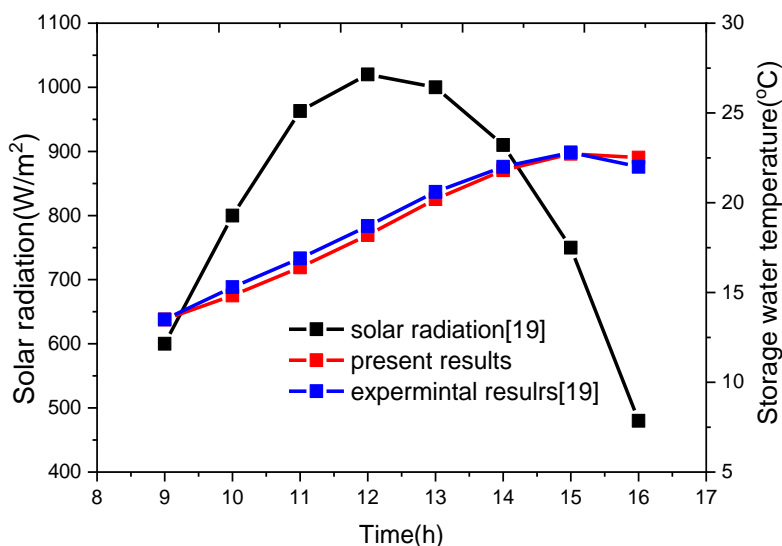


**Figure (4):** Comparison between the standard collector's storage temperature and the previous findings.

### 6. Results and Discussion

The next sections provide the numerical findings from the 3-D unsteady collector configurations with dimensions of [length H of 1 m, width W of 1 m, and depth Z of 1 m] that are displayed in Figure (1). On a typical, clear day in May, the operational weather conditions in Kufa, Iraq, as shown in Table (3), can alter the sun's power, the surrounding temperature, and the wind speed at any time. Every hour, the system performance parameters were achieved. These comprised total energy stored, velocity dispersion, average storage temperature, and thermal efficiency. The typical outcomes are shown as follows.

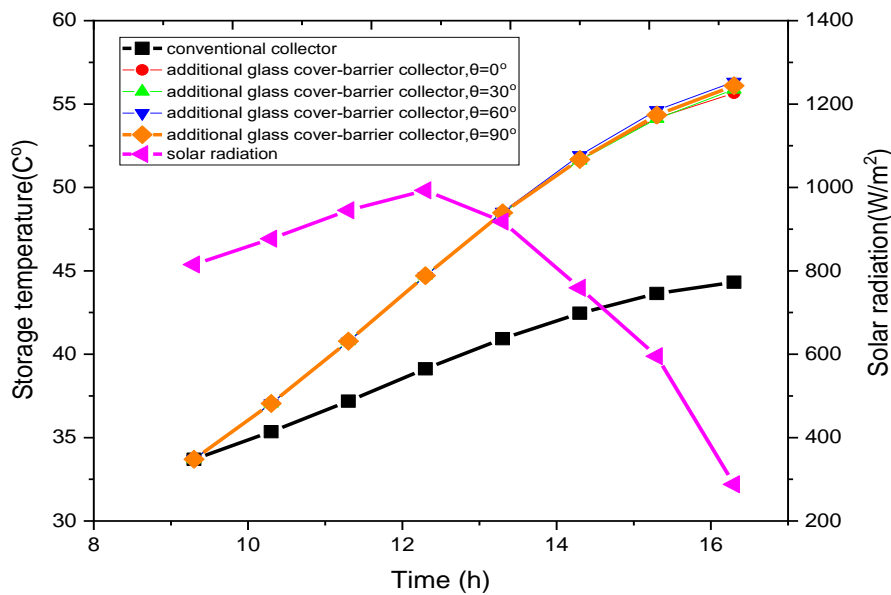
#### 6.1. System Temperatures

Figure (5) demonstrates a variance in the storage collectors' average storage temperature on an ordinary, sunny day in May. At midday, when it reaches its peak, the amount of sunlight progressively increases before beginning to progressively drop. The average temperature for storage. is seen to increase over time as heating takes place, peaking for all collectors towards the end of the operation period. This happened because there was

a greater amount of usable energy delivered to the water due to the net energy absorbed being larger than the heat losses. Although their reported values are different, this tendency corresponds to the hourly rise indicated by [20] and [21]. The water heated up to a temperature of 56.3 °C when the water's original temperature was  $T_i$  was 33.3 °C, for average ambient temperatures of 38.8 °C, and the mean wind velocity of 0.15 m/s, clearly demonstrating that the additional glass cover-barrier storage collector with  $\theta=60^\circ$  experiences the highest system heating than conventional collector. The maximum storage temperature value is affected by a wide range of variables. Among them are the temperature of the inlet water, heat losses. The amount of sun radiation, the surrounding temperature, humidity, wind speed, and other meteorological factors at the moment.

**Table (3):** Weather conditions on 9th May on Kufa-Iraq.

Time(h)	Solar radiation $S$ ( $W/m^2$ )	Ambient temperature $T_{am}$ ( $C^\circ$ )	Wind speed $v_{wi}$ (m/sec)
9.30	815	33.7	0.1
10.30	877	35.4	0.2
11.30	945	38	0.1
12.30	993	43.2	0.3
13.30	918	42.5	0.2
14.30	759	40	0.1
15.30	595	39.3	0.1
16.30	288	38.3	0.1



**Figure (5):** Variation of average storage temperature and solar radiation for the suggested solar storage collector.

The variance in absorber surface temperature for the current models is shown in Figure (6). The temperature of the extra glass cover-barrier collector absorber surface is higher than that of the regular model. Due of the greater absorber temperature, the additional glass cover-barrier storage collector model's mean storage temperature is higher than that of the traditional collector. When adjusting the barrier's inclination angle  $\theta$  from  $0^\circ$  to  $90^\circ$ , it can be noted that storage and absorber temperatures for the additional glass cover-barrier storage collector are roughly consistent.

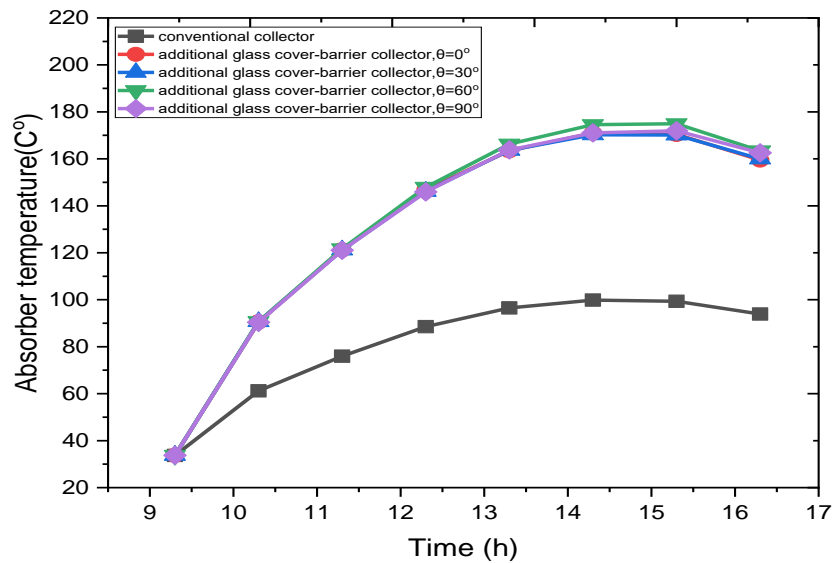


Figure (6): Variation of average absorber temperature for the suggested solar storage collector.

### 6.2. Velocity and Temperature Distribution

The 3D simulation model, which additionally lets one see the streamlines' courses, gives further details regarding the water's convection motion inside the collectors. In three dimensions, Figure (7) shows the distributions of velocity in the suggested collectors at 12.30 PM. As depicted in this diagram, the additional glass cover-barrier storage collector has numerous circulation cells (vortexes) compared to the standard collector's single cell. The density of the water varies naturally as a result of the heat transfer brought on by absorbed solar radiation. Due to the buoyancy effect, the water flows naturally in respect to the inner collecting walls. The phenomenon persists as long as there is an influx of solar radiation. Buoyancy forces cause water molecules to climb to the top of a heated, sloped absorber surface before turning them downward to the collector's back side. Figure (8) shows the distribution of temperature in the collectors at 12.30 PM. Thermal gradients in the water volume are quite significant. The temperature was highest in the added glass cover-barrier storage collector.

### 6.3. Storage Energy and Efficiency

The stored energy is one of the most important factors in determining how well a solar storage collector works. One of the most important factors to take into account when choosing a solar storage collector is the storage energy. After determining the average storage temperature and the rate of growth throughout the process time, the following equation can be used to estimate the stored or usable energy  $Q_{st}$  [22]:

$$Q_{st} = m_w C_w (T_f - T_s) \quad (6)$$

Where:  $m_w$  Mass of water in the collector [kg],  $C_w$  Water specific heat [J/kg K],  $T_f$  Water temperature inside collector in the final hour [°C], and  $T_s$  Water temperature of the collector at the start of the hour [°C]. The variation in the average water temperature over the course of operation determines heat gain amount of. The variation in the energy which was stored in the recommended collector devices is shown in Figure (9). After 13.30 PM, the amount of energy stored attains its maximum and starts to decrease. This is due to the significant rise in net energy absorbed and the comparatively low heat losses from the collector to the surrounding atmosphere. The additional glass cover-barrier storage collector design was also reported to have a higher rate of storage energy than the previous type. While the greatest value for a conventional storage collector was 1007.06 W, the highest value for an additional glass cover-barrier storage collector with an angle of 60° was 2065.6 W. Instantaneous efficiency ( $\eta_{ins}$ ) is the ratio of a collector's useful gain to incident solar energy during a certain time period [22, 23]:

$$\eta_{ins} = \frac{Q_{st}}{A_a \cdot \tau_g \cdot \tau_{ag} \cdot \alpha_{ab} \cdot \Sigma S} \quad (7)$$



Using the above equation [7], Figure (10) shows the hourly fluctuation in thermal efficiency of the storage collectors. Thermal efficiency varies in a manner that is strongly correlated with stored energy varies. The top instantaneous efficiency for additional glass cover-barrier storage collector is at 13.30 PM with an angle of  $60^\circ$  and a value of 58.3%, while the peak for conventional collector is 28.4%. This increase in efficiency of additional glass cover-barrier storage collector return to the restricted air between a double glass covers, which reduces heat transfer to the surroundings.

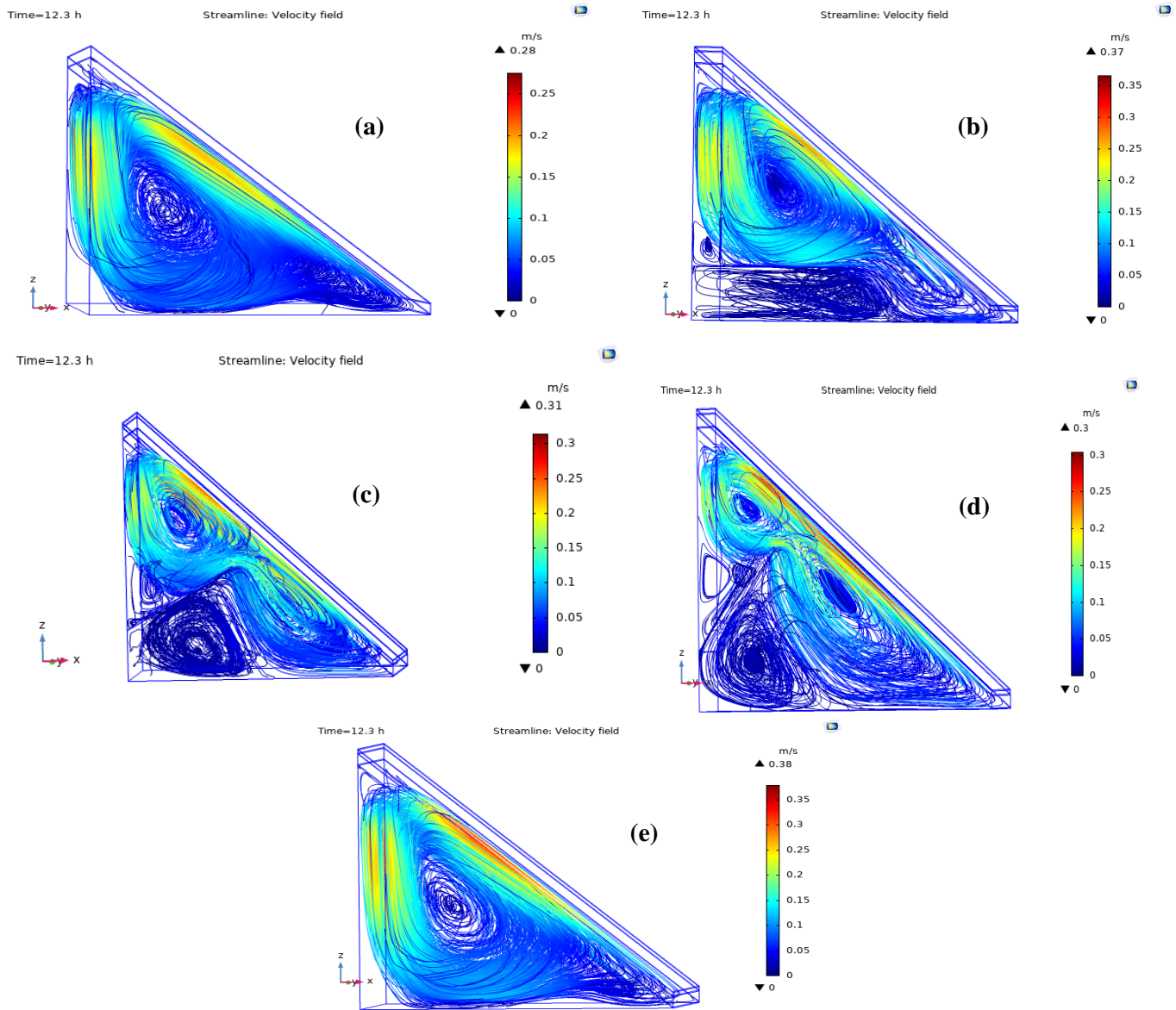


**Figure (7):** Streamlines patterns for the suggested solar storage collector at time 12.30 PM.

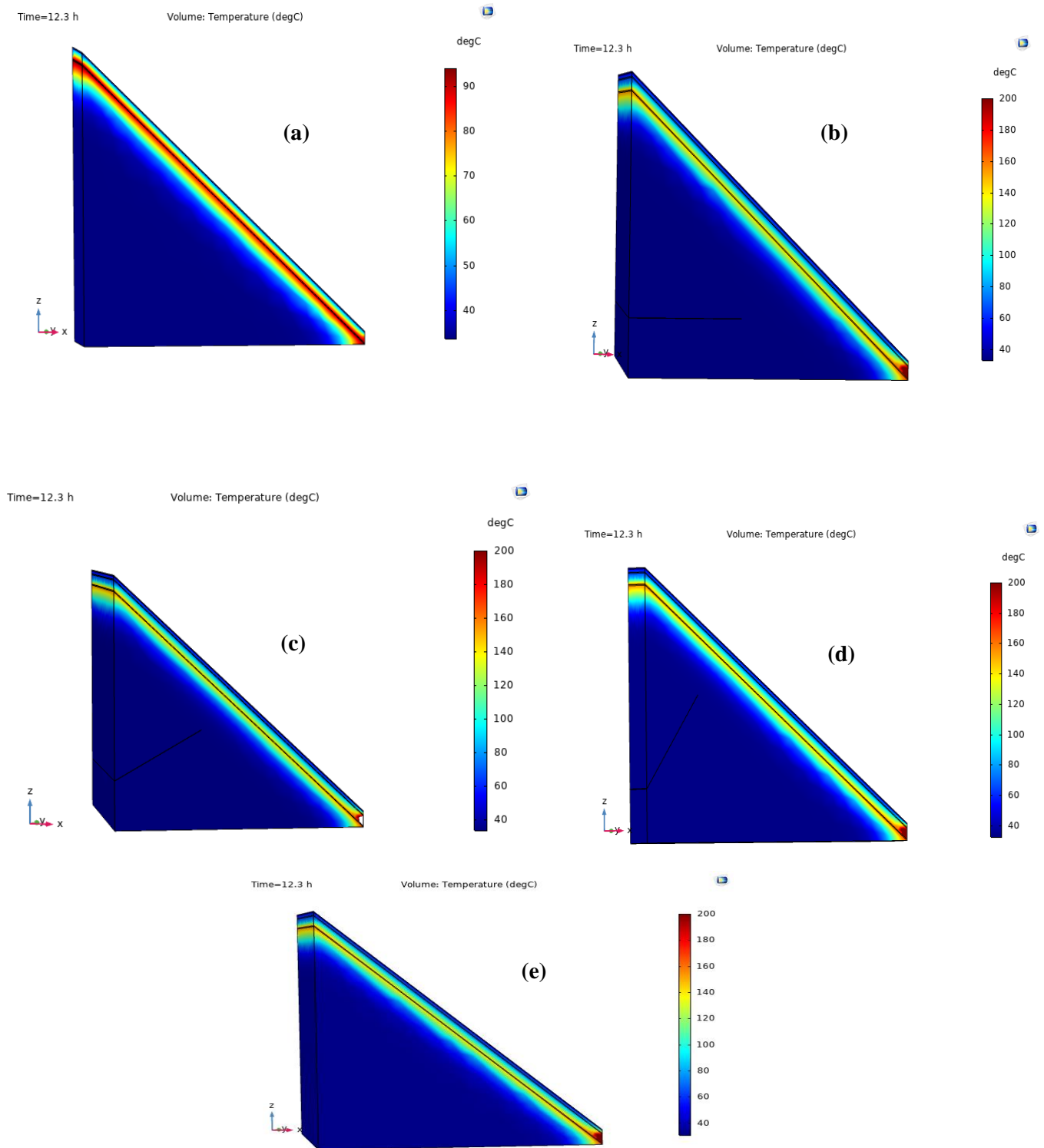


**Figure (8):** Temperature distribution for the suggested solar storage collector at time 12.30 PM.

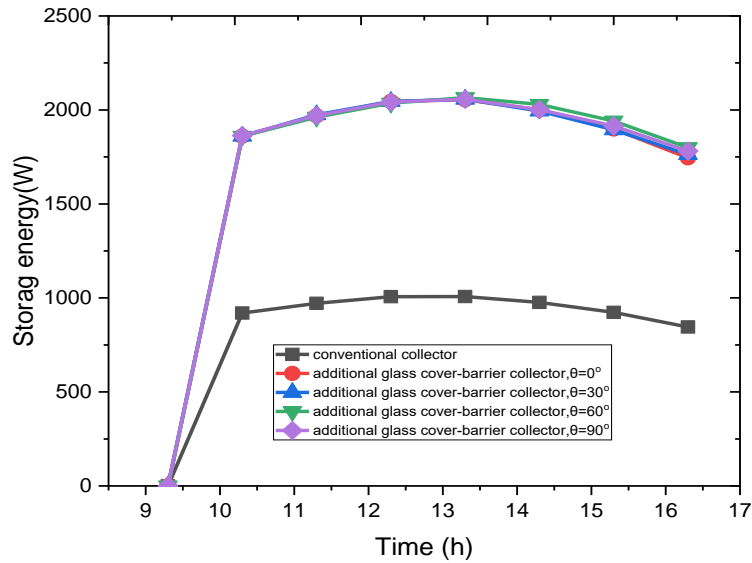


Figure (9): Hourly variation of storage energy of the suggested solar storage collector.

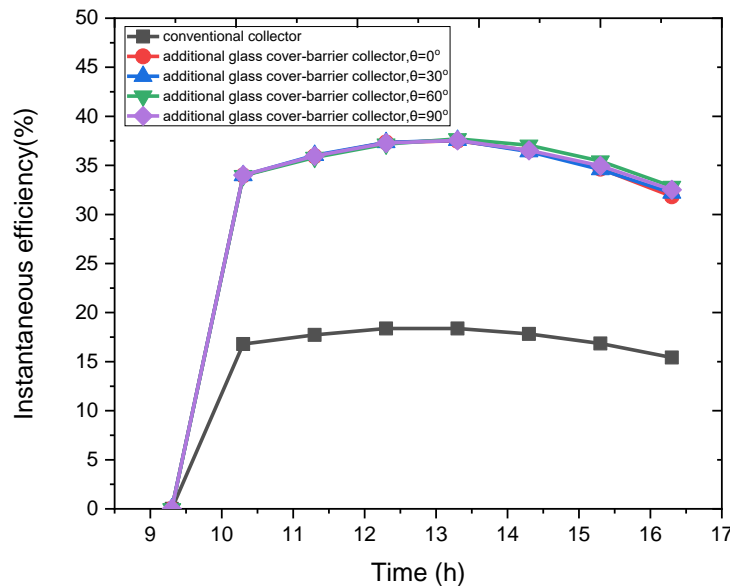


Figure (10): Hourly variation of instantaneous efficiency for the suggested solar storage collector.

## 7. Conclusions

The study's major objective was to develop a CFD model for a modified rectangular solar storage collector in order to use it to enhance the collector's performance. With this model, a CFD simulation of the unsteady system has been constructed in COMSOL. The current numerical findings and the prior numerical and experimental data have been linked. From the above results, the storage water temperature can reach a maximum value of 56.3 °C at the end period of operation when the initial water temperature was 33.3 °C. Moreover, compared to the conventional storage collector, the additional glass cover-barrier storage collector design performed better with higher rate of storage energy were noted in additional glass cover-barrier storage collector model. The maximum value of stored energy was 2065.6 W while it is 1007.06 W in a traditional storage collector. Also, it was discovered that the conventional storage collector storage collector's instantaneous efficiency less than the efficiency of the additional glass cover-barrier storage collector with a value of 28.4% as compared with a 58.3% for additional glass cover-barrier storage collector. Finally, change the angle of barrier inside storage collector saw a slight improvement in the effectiveness of additional glass cover-barrier storage collector.

**Conflict of Interest:** The authors declare that there are no conflicts of interest associated with this research project. We have no financial or personal relationships that could potentially bias our work or influence the interpretation of the results.

## References

- [1] N. Mokhlif, M. Eleiwi and T. Yassen “Experimental evaluation of a solar water heater integrated with a corrugated absorber plate and insulated flat reflectors”, *AIMS Energy*, vol. 11, no. 3, pp. 522–539, 2023.
- [2] D. Mutasher and A. Mola “Experimental investigation of solar water heater type helical coil vertical collector with concentrator”, *Journal of Mechanical Engineering Research and Developments*, vol. 43, no. 6, pp. 381-387, 2020.
- [3] J. Duffie, and W. Beckman, “Solar Engineering of Thermal Processes”. 4<sup>th</sup> ed. John Wiley & Sons, Inc, 2013.
- [4] M. Smyth, C. Eames, and B. Norton, “Integrated collector storage solar water heaters”, *Renewable and Sustainable Energy Reviews*, vol. 10, pp. 503–538, 2006.
- [5] M. Suha, “An Experimental Study on Improving the Thermal Storage of ICWS.” *International Journal of Scientific & Engineering Research*, vol. 5, no. 9, pp. 138-143, 2014.
- [6] O. Khalil, A. Hassen “Principle of Renewable Energies”, 1<sup>st</sup> ed., Foundation of Technical Education, Baghdad, 2011.
- [7] O. Khalil, A. Hassen, and O. Majeed “Effect of the Shape Surface of Absorber Plate on Performance of Built-In Storage Solar Water Heater.” *Journal of Iraqi Desert Studies* vol. 2, no. 2, pp. 69-80, 2010.
- [8] A. Joudi, I. Hussein, and A. Farhan, “Computational model for a prism shaped storage solar collector with a right triangular cross section”, *Energy Conversion and Management*, vol. 45 no. 3, pp. 391–409, 2004.
- [9] O. Ahmed, Kh. Hamada, A. Salih et al, “A state of the art review of PV-Trombe wall system: Design and applications”, *Environmental progress and sustainable energy*, pp. 1–16.
- [10] O. Ahmed, “A numerical and experimental investigation for a triangular storage collector”, *Solar Energy*, no. 171, pp. 884–892, 2018.
- [11] A. Khalil “Experimental and numerical investigation of cylindrical storage collector (case study)”, *Case Studies in Thermal Engineering*, vol. 10, pp. 362–369, 2017.
- [12] K. Ahmed, “Assessment of the Performance for a New Design of Storage Solar Collector”, *International journal of renewable energy research*, vol. 8, no. 1, pp. 250–257, 2018.
- [13] N. Mokhlif, M. Eleiwi and T. Yaseen “Experimental evaluation of a solar water heater integrated with a corrugated absorber plate and insulated flat reflectors.” *AIMS Energy* vol. 11, no. 3, pp. 522–539, 2023.
- [14] N. Mokhlif, M. Eleiwi and T. Yaseen “Experimental investigation of a double glazing integrated solar water heater with corrugated absorber surface.” *Materials Today Proceedings*, vol. 42, no. 5, pp. 2742–2748, 2020.
- [15] H. Buchberg, I. Catton, and D. Edwards, “Natural convection in enclosed spaces- A review of application of solar collection,” *Trans of the ASME, J. of Heat transfer*, vol. 98, pp. 182-188, 1976.
- [16] M. Slimani, M. Amirat, I. Kurucz, S. Bahria, and et al. “A detailed thermal-electrical model of three photovoltaic/thermal (PV/T) hybrid air collectors and photovoltaic (PV) module: Comparative study under Algiers climatic conditions”, *Energy Conversion and Management*, vol. 133, pp. 458-476, 2016.
- [17] COMSOL Multiphysics Reference Manual, Version 5.0, COMSOL software license, 2015.
- [18] M. Koffi, H. Andoh, P. Gbaha, and et al. “Theoretical and experimental study of solar water heater with internal exchanger using thermosiphon system”, *Energy Convers. Manag.* vol. 49, pp. 2279–2290, 2008.
- [19] O. Ahmad “Numerical and Experimental Performance Analysis for a Novel Design of Storage Solar Collectors”, Ph.Sc. Thesis, Al- Nahrain University, 2006
- [20] W. Alawi, “Numerical and experimental study of the solar collector storage pyramidal with right angle”, M.Sc. Thesis, University of Technology, 2004.
- [21] H. Wisam, “A Simple Design Solar Water Heater” *AlTaqani Journal*, vol. 21, pp. 27-38, 2008.
- [22] A. Abdullah, O. Ahmed and Z. Ali, “Performance analysis of the new design of photovoltaic/storage solar collector”, *Energy Storage*. 2019.
- [23] S. Mohammed “An Experimental Study on Improving the Thermal Storage of ICWS”, *International Journal of Scientific & Engineering Research*, vol. 5, no. 9, pp. 138-143, 2014.